

Free-breathing R_2^* Mapping in the Entire Placenta During Early Gestation Using 3D Stack-of-Radial MRI at 3 T: Investigation of Spatial and Temporal Variation

Tess Armstrong^{1,2}, Dapeng Liu¹, Thomas Martin^{1,2}, Cass Wong¹, Irish Del Rosario³, Sherin U. Devaskar⁴, Carla Janzen⁵, Teresa Chanlaw⁴, Rinat Masamed¹, Kyunghyun Sung^{1,2}, and Holden H. Wu^{1,2}

¹Radiological Sciences, University of California Los Angeles, Los Angeles, CA, United States, ²Physics and Biology in Medicine, University of California Los Angeles, Los Angeles, CA, United States, ³Epidemiology, University of California Los Angeles, Los Angeles, CA, United States, ⁴Pediatrics, David Geffen School of Medicine at UCLA, University of California Los Angeles, Los Angeles, CA, United States, ⁵Obstetrics and Gynecology, David Geffen School of Medicine at UCLA, University of California Los Angeles, Los Angeles, CA, United States

Synopsis

Current methods for detecting ischemic placental disease are either invasive or have low sensitivity. MRI can be used to non-invasively characterize tissue hypoxia with R_2^* mapping. However, conventional Cartesian MRI methods are sensitive to motion artifacts due to maternal and fetal motion. In this study, a non-Cartesian free-breathing 3D stack-of-radial MRI technique (FB radial) for R_2^* mapping in the placenta during early gestation was investigated at 3T. In 20 subjects, placental R_2^* range, accuracy, repeatability, spatial variation, and temporal variation were analyzed. Results demonstrate that FB radial is an accurate and repeatable technique for R_2^* mapping in the entire placenta.

Introduction

Ischemic placental disease (IPD) can lead to pre-eclampsia, fetal growth restriction, preterm labor, and spontaneous abortion^(1,2). Detection of IPD during early gestation may enable earlier intervention to improve outcomes. Current methods to detect IPD include invasive chorionic villous sampling (CVS)⁽³⁾ and non-invasive uterine artery Doppler (UA Doppler). However, CVS can cause complications and UA Doppler has low sensitivity during early gestation^(4,5). MRI may be able to detect IPD by characterizing hypoxia with R_2^* maps⁽⁶⁻⁸⁾. However, conventional R_2^* mapping techniques employ Cartesian sampling, which is sensitive to coherent aliasing artifacts caused by maternal respiratory motion, uterine contractions, and fetal motion. Therefore, previous studies have used 2D breath-held Cartesian techniques, which limits the placental coverage, potentially causing sampling bias and reducing repeatability⁽⁶⁻⁸⁾. 3D stack-of-radial trajectories have greater robustness to motion artifacts, allowing for free-breathing MRI⁽⁹⁾. In this work, we propose and evaluate a free-breathing (FB) 3D stack-of-radial technique^(10,11) for quantifying R_2^* in the entire placenta at 3T during early gestation.

Methods

FB Radial Sequence A bipolar multiecho gradient echo 3D stack-of-radial sequence with golden-angle ordering (FB radial) (**Fig. 1a**)^(10,11) was developed to improve robustness to motion and enable R_2^* mapping of the entire placenta.

Experimental Design A phantom with an R_2^* range of 5-70s⁻¹ was scanned with FB radial and a multiecho gradient echo Cartesian sequence (Cartesian) with matched imaging parameters (**Table 1**). With IRB approval and after obtaining informed consent, twenty pregnant subjects (age=35.41±3.41years) without any known pregnancy complications were enrolled. Placenta scans were acquired with subjects in the feet-first supine position at 3T (Skyra/Prisma, Siemens) using 2D T₂ HASTE⁽¹²⁾ and FB radial sequences (**Table 1**). Each subject had scans performed at two gestational age (GA) intervals of 14-18 weeks and 19-23 weeks (**Fig. 1a**). Two FB radial scans were acquired back-to-back in the same session to assess repeatability.

Reconstruction FB radial and Cartesian images were reconstructed offline. FB radial reconstruction included gradient calibration and correction⁽¹¹⁾. Signal model fitting for both FB radial and Cartesian was performed⁽¹³⁻¹⁵⁾, a 7-peak fat model⁽¹⁶⁾, and a single effective R_2^* per voxel⁽¹⁷⁻¹⁹⁾.

Analysis T₂ HASTE images were registered to FB radial images using Advanced Normalization Tools software⁽²⁰⁾. The entire placenta was contoured on registered T₂ HASTE images and regions of interest (ROIs) were copied to FB radial images and R_2^* maps (**Fig. 1b**). FB radial R_2^* repeatability was assessed by calculating the mean difference (MD), absolute mean difference (MD_{abs}), and coefficient of repeatability (CR). R_2^* from the FB radial scans performed at the two GA intervals were used to determine normalized mean R_2^* at 16 and 21 weeks GA, mean coefficient of variation (CV) to assess spatial variation, and mean change in R_2^* over GA (ΔR_2^*) to assess temporal variation. Subjects were analyzed together and also by placenta implantation position (anterior or posterior). A two-sided t-test was performed to compare differences in mean R_2^* , CV, and ΔR_2^* between anterior and posterior placenta positions (P<0.05 considered significant).

Results

FB radial provided accurate and repeatable R_2^* quantification in a phantom (**Fig. 2**) compared to a reference Cartesian method. In pregnant subjects, images were acquired without substantial motion or undersampling artifacts using FB radial (**Fig. 3**). FB radial R_2^* had a range of 9-21s⁻¹ and demonstrated repeatability with MD<1.2s⁻¹, MD_{abs}<1.75s⁻¹ and CR<6s⁻¹. The normalized mean R_2^* at 16 and 21 weeks, CV, and ΔR_2^* are shown in **Table 2**. Higher CR and CV (P<0.05) were observed for the posterior placentas. Mean R_2^* for posterior placentas tended to decrease as a function of GA, while mean R_2^* tended to increase for anterior placentas.

Discussion

FB radial R_2^* mapping demonstrated accuracy and repeatability in a phantom, and good repeatability in pregnant subjects. FB radial improves patient comfort during MRI by not requiring breath-holding and accommodating maternal and fetal motion. By acquiring 3D R_2^* maps throughout the entire placenta, FB radial may reduce sampling bias and characterize spatial variation. FB radial R_2^* had better repeatability in the first session compared to the second one, particularly for posterior placentas. Variations may be due to fetal motion, which was observed in some repeated scans. Ongoing work will include more subjects to achieve necessary power for significance and further investigation of spatial and temporal variation. This study contributes to the understanding of R_2^* in normal pregnancies during early gestation and may be extended to study IPD and abnormal pregnancies for early detection and intervention. Previous studies at 1.5T during later GA showed significant R_2^* changes in abnormal pregnancies^(6,7).

Conclusion

FB radial can provide accurate and repeatable R_2^* mapping in the entire placenta of pregnant subjects at 3T. This technique allows for increased comfort and may support early detection and monitoring of ischemic placental disease.

Acknowledgements

This work acknowledges the use of the ISMRM Fat-Water Toolbox (<http://ismrm.org/workshops/FatWater12/data.htm>). This work was funded by the grant NICHD U01-HD087221. The authors thank Sitaram S. Vangala at UCLA for helpful discussions.

References

1. Kingdom JCP, Kaufmann P. Oxygen and placental villous development: Origins of fetal hypoxia. *Placenta* 1997;18:613–621. doi: 10.1016/S0143-4004(97)90000-X.
2. Parks WT. Placental hypoxia: The lesions of maternal malperfusion. *Semin. Perinatol.* 2015;39:9–19. doi: 10.1053/j.semperi.2014.10.003.
3. Rhoads GG, Jackson LG, Schlesselman SE, et al. The safety and efficacy of chorionic villus sampling for early prenatal diagnosis of cytogenetic abnormalities. *N Engl J Med* 1989;320:609–617. doi: 10.1056/NEJM198903093201001.
4. Bamfo JE a K, Odibo AO. Diagnosis and management of fetal growth restriction. *J. Pregnancy* 2011;2011:640715. doi: 10.1155/2011/640715.
5. Khong SL, Kane SC, Brennecke SP, Da Silva Costa F. First-trimester uterine artery doppler analysis in the prediction of later pregnancy complications. *Dis. Markers* 2015;2015. doi: 10.1155/2015/679730.
6. Sinding M, Peters DA, Frøkjær JB, Christiansen OB, Petersen A, Uldbjerg N, Sørensen A. Prediction of low birth weight: Comparison of placental T_2^* estimated by MRI and uterine artery pulsatility index. *Placenta* 2017;49:48–54. doi: 10.1016/j.placenta.2016.11.009.
7. Sinding M, Peters D a., Frøkjær JB, Christiansen OB, Petersen A, Uldbjerg N, Sørensen A. Placental T_2^* measurements in normal pregnancies and in pregnancies complicated by fetal growth restriction. *Ultrasound Obstet. Gynecol.* 2015. doi: 10.1002/uog.14917.
8. Huen I, Morris DM, Wright C, Parker GJM, Sibley CP, Johnstone ED, Naish JH. R_1 and R_2^* changes in the human placenta in response to maternal oxygen challenge. *Magn. Reson. Med.* 2013;70:1427–33. doi: 10.1002/mrm.24581.
9. Block KT, Chandarana H, Milla S, et al. Towards routine clinical use of radial stack-of-stars 3D gradient-echo sequences for reducing motion sensitivity. *J. Korean Soc. Magn. Reson. Med.* 2014;18:87–106. doi: 10.13104/jksmrm.2014.18.2.87.
10. Armstrong T, Liu D, Martin T, et al. Free-breathing R_2^* Characterization of the Placenta During Normal Early Gestation Using a Multiecho 3D Stack-of-Radial Technique. In: *In Proc. Intl. Soc. Mag. Reson. Med.* ; 2017. p. 117.
11. Armstrong T, Dregely I, Stemmer A, Han F, Natsuaki Y, Sung K, Wu HH. Free-breathing liver fat quantification using a multiecho 3D stack-of-radial technique. *Magn. Reson. Med.* 2017. doi: 10.1002/mrm.26693.
12. Patel MR, Klufas RA, Alberico RA, Edelman RR. Half-fourier acquisition single-shot turbo spin-echo (HASTE) MR: Comparison with fast spin-echo MR in diseases of the brain. *Am. J. Neuroradiol.* 1997;18:1635–1640.
13. Hernando D, Kellman P, Haldar JP, Liang Z-P. Robust water/fat separation in the presence of large field inhomogeneities using a graph cut algorithm. *Magn. Reson. Med.* 2010;63:79–90. doi: 10.1002/mrm.22177.
14. ISMRM Fat Water Toolbox. 2012.
15. Gleich DF. *Models and Algorithms for PageRank Sensitivity*. Stanford University; 2009.
16. Ren J, Dimitrov I, Sherry AD, Malloy CR. Composition of adipose tissue and marrow fat in humans by 1H NMR at 7 Tesla. *J. Lipid Res.* 2008;49:2055–2062. doi: 10.1194/jlr.D800010-JLR200.
17. Horng DE, Hernando D, Hines CDG, Reeder SB. Comparison of R_2^* correction methods for accurate fat quantification in fatty liver. *J. Magn. Reson. Imaging* 2013;37:414–22. doi: 10.1002/jmri.23835.
18. Horng DE, Hernando D, Reeder SB. Quantification of liver fat in the presence of iron overload. *J. Magn. Reson. Imaging [Internet]* 2017. doi: 10.1002/jmri.25382.

20. Advanced Normalization Tools (ANTs).

Figures

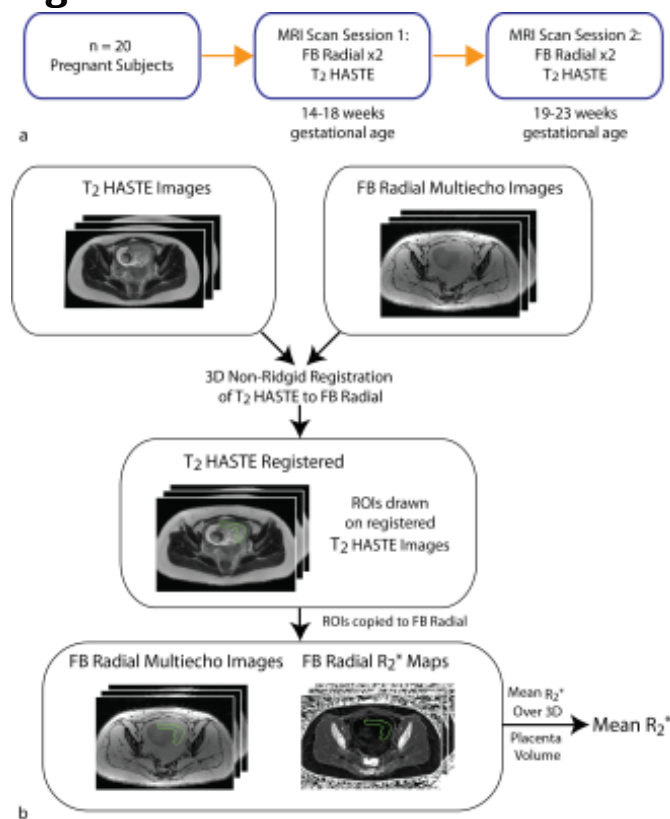


Figure 1: (a) N=20 pregnant subjects were recruited for this study and underwent an MRI scan session acquiring FB radial and T₂ HASTE images in the range of 14-18 weeks and 19-23 weeks gestational age. FB radial was acquired twice to assess repeatability. (b) T₂ HASTE images were registered to FB radial images and the placenta was contoured with regions of interest (ROIs) drawn throughout the entire placenta volume. ROIs were then copied to FB radial images and R₂^{*} maps to determine the mean R₂^{*}.

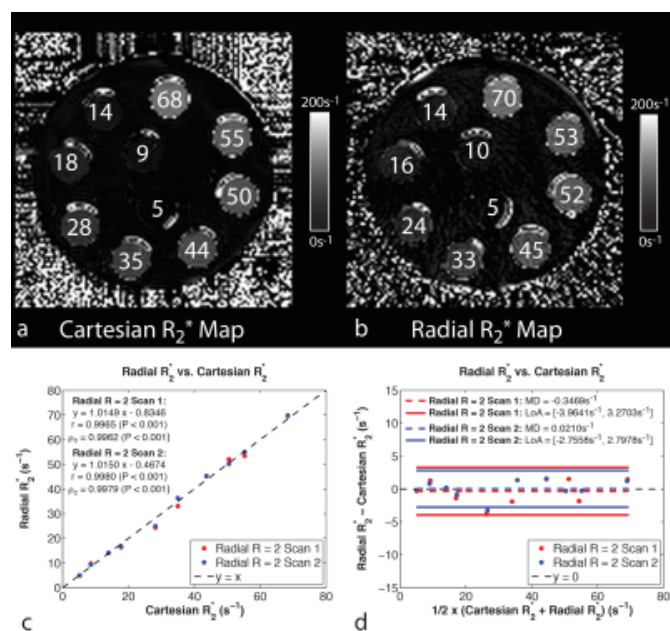


Figure 2: The ferumoxytol phantom with a R₂^{*} range of 5-70s⁻¹. (a) Cartesian and (b) radial R₂^{*} maps (s⁻¹) acquired in the axial orientation. The (c) linear correlation and (d) Bland-Altman analysis plots showed excellent agreement between radial scan 1 and scan 2 and Cartesian. Radial scan 1 and scan 2 were acquired back-to-back in the same session to assess repeatability.

Imaging Parameters	T ₂ HASTE	FB Radial
Number of Echoes (TE)	1	12
First TE (ms)	92	1.23
ΔTE (ms)	N/A	1.23
Last TE (ms)	N/A	14.76
Echo Train Length	70	N/A
TR (ms)	3000	15.90
Matrix (N _x x N _y)	272 x 512	224 x 224
Field of View (mm _x x mm _y)	265 x 500	380 x 380
Resolution (mm _x x mm _y)	0.974 x 0.976	1.696 x 1.696
Slice Thickness (mm)	5	4
Number of Slices	45-60	44
Radial Spokes	N/A	176 (R = 2)
Flip Angle (degrees)	150	5
Bandwidth (Hz/pixel)	390	1175
Scan Time (min:s)	2:06	3:16*

Table 1: FB radial and T₂ HASTE MRI acquisition parameters for the placenta scans. R denotes the undersampling factor. *The gradient calibration scan time of 61s is included.

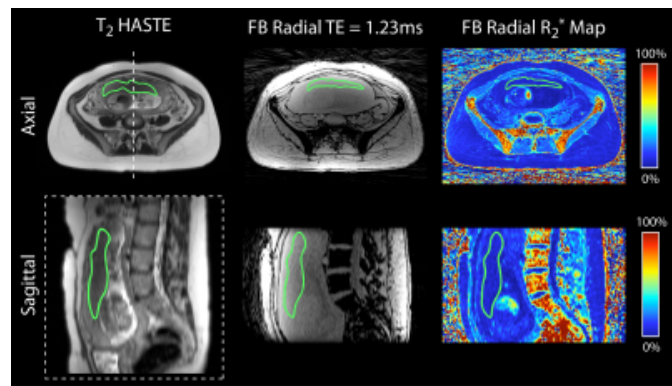


Figure 3: T₂ HASTE, FB radial TE = 1.23 and R₂* maps (s⁻¹) of the placenta (green contours) from a representative subject in the axial and sagittal reformat orientations. The dashed line indicates the position along the right-left direction for the sagittal orientation reformat (dashed box).

Placenta Temporal and Regional Variation						
	Mean R ₂ * 16 weeks (s ⁻¹)	Mean R ₂ * 21 weeks (s ⁻¹)	ΔR ₂ * (s ⁻²)	CV 14-18 weeks	CV 19-23 weeks	
All Subjects (n = 20)	12.92s ⁻¹ ± 2.54s ⁻¹	13.38s ⁻¹ ± 1.83s ⁻¹	0.09s ⁻² ± 0.66s ⁻²	0.65 ± 0.15	0.57 ± 0.14	
Anterior Placenta (n = 9)	12.78s ⁻¹ ± 1.99s ⁻¹	14.21s ⁻¹ ± 1.17s ⁻¹	0.28s ⁻² ± 0.56s ⁻²	0.57 ± 0.13*	0.49 ± 0.10*	
Posterior Placenta (n = 11)	13.03s ⁻¹ ± 3.01s ⁻¹	12.70s ⁻¹ ± 2.03s ⁻¹	-0.07s ⁻² ± 0.72s ⁻²	0.71 ± 0.14*	0.64 ± 0.14*	
FB Radial R ₂ * Repeatability Analysis						
	14-18 Weeks GA			19-23 Weeks GA		
	MD (s ⁻¹)	MD _{abs} (s ⁻¹)	CR (s ⁻¹)	MD (s ⁻¹)	MD _{abs} (s ⁻¹)	CR (s ⁻¹)
All Subjects (n = 20)	0.02s ⁻¹	0.93s ⁻¹	3.40s ⁻¹	0.73s ⁻¹	1.38s ⁻¹	4.97s ⁻¹
Anterior Placenta (n = 9)	0.05s ⁻¹	0.82s ⁻¹	3.07s ⁻¹	0.15s ⁻¹	0.95s ⁻¹	3.35s ⁻¹
Posterior Placenta (n = 11)	-0.01s ⁻¹	1.02s ⁻¹	3.79s ⁻¹	1.20s ⁻¹	1.73s ⁻¹	5.80s ⁻¹

Table 2: The normalized mean R₂* at 16 weeks and 21 weeks gestational age, temporal change in R₂* (ΔR₂*) and spatial coefficient of variation (CV) for all subjects and subjects grouped by placenta implantation position (anterior or posterior). Mean R₂*, ΔR₂* and CV are reported as mean ± standard deviation between subjects. For repeatability analysis, the mean difference (MD), absolute mean difference (MD_{abs}) and coefficient of repeatability (CR) are reported for each GA range. *Statistically significant differences in CV between anterior and posterior placenta implantation position (P < 0.05).